

Exponential Growth and Filamentary Structure of Nonlinear Ballooning Instability ¹

Ping Zhu

in collaboration with

C. C. Hegna and C. R. Sovinec

University of Wisconsin-Madison

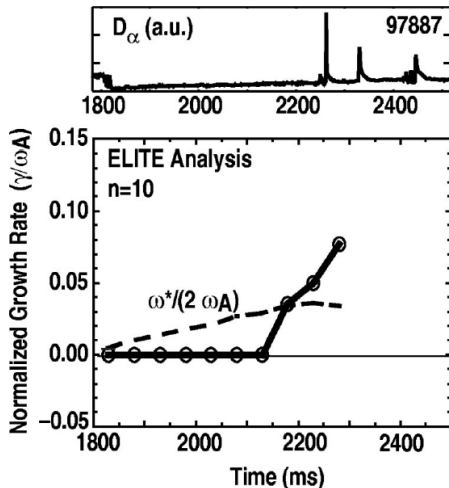
Sherwood Conference
Denver, CO
May 5, 2009

¹Research supported by U.S. Department of Energy.

Close correlation found between onset of type-I ELMs and peeling-ballooning instabilities

- ▶ Breaching of P-B stability boundary correlated to ELM onset (DIII-D)

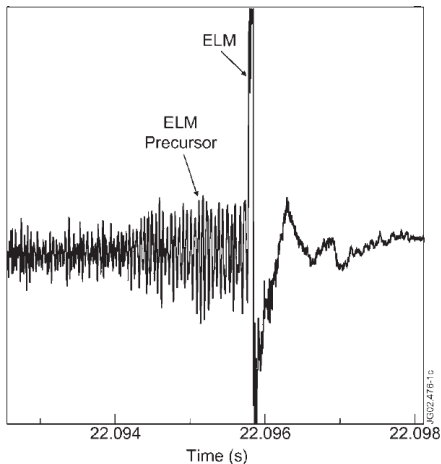
[Snyder *et al.*, 2002].



Close correlation found between onset of type-I ELMs and peeling-ballooning instabilities

- ▶ P-B modes were identified in ELM precursors (JET)

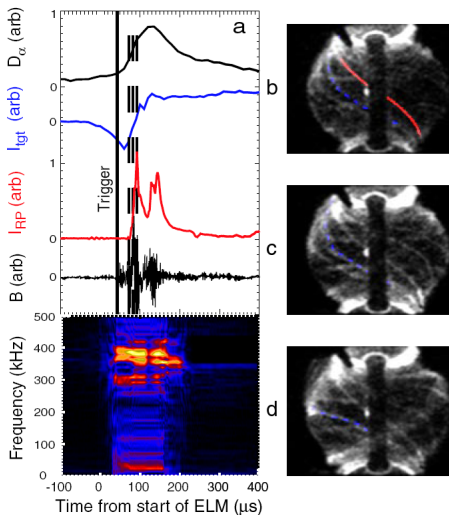
[Perez *et al.*, 2004].



Close correlation found between onset of type-I ELMs and peeling-ballooning instabilities

- ▶ Filament structures persist after ELM onset (**MAST**)

[Kirk *et al.*, 2006].



Causal relation between ballooning instability and ELM dynamics remains unclear

- ▶ Questions on ELM dynamics:
 - ▶ Is ELM onset triggered by ELM precursors? How?
 - ▶ Is ballooning instability responsible for ELM precursor or ELM itself?

Causal relation between ballooning instability and ELM dynamics remains unclear

- ▶ Questions on ELM dynamics:
 - ▶ Is ELM onset triggered by ELM precursors? How?
 - ▶ Is ballooning instability responsible for ELM precursor or ELM itself?
- ▶ Questions on ballooning instability ([this talk](#)):
 - ▶ How fast does it grow in nonlinear stage?
 - ▶ How does ballooning mode structure evolve nonlinearly?

Different nonlinear regimes of ballooning instability can be characterized by the relative strength of nonlinearity ε in terms of n^{-1}

- ▶ Nonlinearity and ballooning parameters

$$\varepsilon \sim \frac{|\xi|}{L_{\text{eq}}} \ll 1, \quad n^{-1} \sim \frac{k_{\parallel}}{k_{\perp}} \sim \frac{\lambda_{\perp}}{\lambda_{\parallel}} \ll 1$$

- ▶ For $\varepsilon \ll n^{-1}$, linear ballooning mode theory [Coppi, 1977; Connor, Hastie, and Taylor, 1979; Dewar and Glasser, 1983]
- ▶ For $\varepsilon \sim n^{-1}$, early nonlinear regime [Cowley and Artun, 1997; Hurricane, Fong, and Cowley, 1997; Wilson and Cowley, 2004; Cowley, Sherwood 2008]
- ▶ For $\varepsilon \sim n^{-1/2}$, **intermediate nonlinear regime** \rightarrow this talk [Zhu, Hegna, and Sovinec, 2006; Zhu *et al.*, 2007; Zhu and Hegna, 2008; Zhu, Hegna, and Sovinec, 2008;]
- ▶ For $\varepsilon \gg n^{-1/2}$, late nonlinear regime; analytic theory under development.

Outline

1. Nonlinear ballooning equations
 - ▶ Formulation
 - ▶ Analytic solution
2. Comparison with NIMROD simulations
 - ▶ Simulation setup
 - ▶ Comparison method
 - ▶ Comparison results
3. Summary and Discussion

A Lagrangian form of ideal MHD is used to develop the theory of nonlinear ballooning instability

$$\begin{aligned} \frac{\rho_0}{J} \nabla_0 \mathbf{r} \cdot \frac{\partial^2 \boldsymbol{\xi}}{\partial t^2} = & -\nabla_0 \left[\frac{\rho_0}{J\gamma} + \frac{(\mathbf{B}_0 \cdot \nabla_0 \mathbf{r})^2}{2J^2} \right] \\ & + \nabla_0 \mathbf{r} \cdot \left[\frac{\mathbf{B}_0}{J} \cdot \nabla_0 \left(\frac{\mathbf{B}_0}{J} \cdot \nabla_0 \mathbf{r} \right) \right] \end{aligned} \quad (1)$$

where $\mathbf{r}(\mathbf{r}_0, t) = \mathbf{r}_0 + \boldsymbol{\xi}(\mathbf{r}_0, t)$, $\nabla_0 = \frac{\partial}{\partial \mathbf{r}_0}$, $J(\mathbf{r}_0, t) = |\nabla_0 \mathbf{r}|$ (2)

The full MHD equation can be further reduced for nonlinear ballooning instability using expansion in terms of ε and n^{-1}

$$\boldsymbol{\xi}(\mathbf{r}_0, t) = \sum_{i=1}^{\infty} \sum_{j=0}^{\infty} \varepsilon^i n^{-\frac{j}{2}} \boldsymbol{\xi}_{(i,j)}(\mathbf{r}_0, t) \quad (3)$$

Nonlinear ballooning expansion is carried out for general magnetic configurations with flux surfaces

- ▶ Clebsch coordinate system (Ψ_0, α_0, l_0)

$$\mathbf{B} = \nabla_0 \Psi_0 \times \nabla_0 \alpha_0 \quad (4)$$

- ▶ Expansions are based on intermediate nonlinear ballooning ordering $\varepsilon \equiv |\xi|/L_{\text{eq}} \sim n^{-1/2} \ll 1$

$$\xi(\sqrt{n}\Psi_0, n\alpha_0, l_0, t) = \sum_{j=1}^{\infty} n^{-j/2} \left(\mathbf{e}_{\perp} \xi_{j/2}^{\Psi} + \frac{\mathbf{e}_{\wedge}}{\sqrt{n}} \xi_{j/2}^{\alpha} + \mathbf{B} \xi_{j/2}^{\parallel} \right) \quad (5)$$

$$J(\sqrt{n}\Psi_0, n\alpha_0, l_0, t) = 1 + \sum_{j=0}^{\infty} n^{-j/2} J_{j/2} \quad (6)$$

where $\mathbf{e}_{\perp} = (\nabla_0 \alpha_0 \times \mathbf{B})/B^2$, $\mathbf{e}_{\wedge} = (\mathbf{B} \times \nabla_0 \Psi_0)/B^2$.

- ▶ The spatial structure of $\xi(\Psi, \alpha, l)$ and $J(\Psi, \alpha, l)$ is ordered to be consistent with linear ideal ballooning theory:
 $\Psi = \sqrt{n}\Psi_0, \alpha = n\alpha_0, l = l_0$.

The linear local ballooning operator will continue to play a fundamental role in the nonlinear dynamics

Linear ideal MHD ballooning mode equation

$$\rho \partial_t^2 \xi = \mathcal{L}(\xi) \quad (7)$$

where local ballooning operator

$$\begin{aligned} \mathcal{L}(\xi) \equiv & \mathbf{B} \cdot \nabla_0 (\mathbf{B} \cdot \nabla_0 \xi) - \nabla_0 (\mathbf{B} \cdot \nabla_0 \mathbf{B}) \cdot \xi \\ & - \mathbf{B} \mathbf{B} \cdot \nabla_0 \left[\frac{1}{1 + \gamma\beta} (\mathbf{B} \cdot \nabla_0 \xi_{\parallel} - 2\kappa \cdot \xi_{\perp}) \right] \\ & - \frac{2\mathbf{B} \cdot \nabla_0 \mathbf{B}}{1 + \gamma\beta} (\mathbf{B} \cdot \nabla_0 \xi_{\parallel} - 2\kappa \cdot \xi_{\perp}) \end{aligned} \quad (8)$$

is an ODE operator along field line, with $\xi = \xi_{\parallel} \mathbf{B} + \xi_{\perp}$.

A set of nonlinear ballooning equations for ξ are described using the linear operator [Zhu and Hegna, 2008]

$$\rho(|\mathbf{e}_\perp|^2 \partial_\alpha \partial_t^2 \xi_{\frac{1}{2}}^\Psi + [\xi_{\frac{1}{2}}, \partial_t^2 \xi_{\frac{1}{2}}]) = \partial_\alpha \mathcal{L}_\perp(\xi_{\frac{1}{2}}^\Psi, \xi_{\frac{1}{2}}^\parallel) + [\xi_{\frac{1}{2}}, \mathcal{L}(\xi_{\frac{1}{2}})], \quad (9)$$

$$\rho B^2 \partial_t^2 \xi_{\frac{1}{2}}^\parallel = \mathcal{L}_\parallel(\xi_{\frac{1}{2}}^\Psi, \xi_{\frac{1}{2}}^\parallel) \quad (10)$$

$$\mathcal{L}_\perp(\xi^\Psi, \xi^\parallel) \equiv \mathbf{e}_\perp \cdot \mathcal{L}(\xi) \quad (11)$$

$$\begin{aligned} &= B \partial_l (|\mathbf{e}_\perp|^2 B \partial_l \xi^\Psi) + 2 \mathbf{e}_\perp \cdot \kappa \mathbf{e}_\perp \cdot \nabla_0 \rho \xi^\Psi \\ &\quad + \frac{2 \gamma \rho \mathbf{e}_\perp \cdot \kappa}{1 + \gamma \beta} \left(B \partial_l \xi^\parallel - 2 \mathbf{e}_\perp \cdot \kappa \xi^\Psi \right), \end{aligned} \quad (12)$$

$$\mathcal{L}_\parallel(\xi^\Psi, \xi^\parallel) \equiv \mathbf{B} \cdot \mathcal{L}(\xi) \quad (13)$$

$$= B \partial_l \left[\frac{\gamma \rho}{1 + \gamma \beta} \left(B \partial_l \xi^\parallel - 2 \mathbf{e}_\perp \cdot \kappa \xi^\Psi \right) \right], \quad (14)$$

$$[\mathbf{A}, \mathbf{B}] \equiv \partial_\Psi \mathbf{A} \cdot \partial_\alpha \mathbf{B} - \partial_\alpha \mathbf{A} \cdot \partial_\Psi \mathbf{B}. \quad (15)$$

The local linear ballooning mode structure continues to satisfy the nonlinear ballooning equations

- ▶ The nonlinear ballooning equations can be rearranged in the compact form

$$\overbrace{[\Psi + \xi^\Psi, \rho |\mathbf{e}_\perp|^2 \partial_t^2 \xi^\Psi - \mathcal{L}_\perp(\xi^\Psi, \xi^\parallel)]}^{\text{nonlinear}} = 0, \quad (16)$$

$$\underbrace{\rho B^2 \partial_t^2 \xi^\parallel - \mathcal{L}_\parallel(\xi^\Psi, \xi^\parallel)}_{\text{linear}} = 0. \quad (17)$$

- ▶ The general solution satisfies

$$\rho |\mathbf{e}_\perp|^2 \partial_t^2 \xi^\Psi = \mathcal{L}_\perp(\xi^\Psi, \xi^\parallel) + N(\Psi + \xi^\Psi, l, t) \quad (18)$$

- ▶ A special solution is the solution of the linear ballooning equations ($N = 0$), for which the nonlinear terms in (16) all vanish.

Implications of the “linear” analytic solution

- ▶ The solution is linear in Lagrangian coordinates, but nonlinear in Eulerian coordinates

$$\boldsymbol{\xi} = \boldsymbol{\xi}_{\text{lin}}(\mathbf{r}_0) = \boldsymbol{\xi}_{\text{lin}}(\mathbf{r} - \boldsymbol{\xi}) = \boldsymbol{\xi}_{\text{non}}(\mathbf{r}).$$

Implications of the “linear” analytic solution

- ▶ The solution is linear in Lagrangian coordinates, but nonlinear in Eulerian coordinates

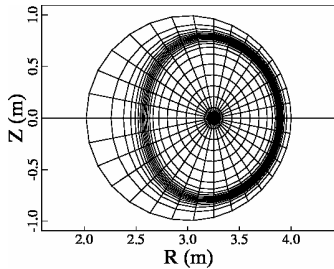
$$\boldsymbol{\xi} = \boldsymbol{\xi}_{\text{lin}}(\mathbf{r}_0) = \boldsymbol{\xi}_{\text{lin}}(\mathbf{r} - \boldsymbol{\xi}) = \boldsymbol{\xi}_{\text{non}}(\mathbf{r}).$$

- ▶ Perturbation developed from linear ballooning instability should continue to
 - ▶ grow exponentially
 - ▶ maintain filamentary spatial structure

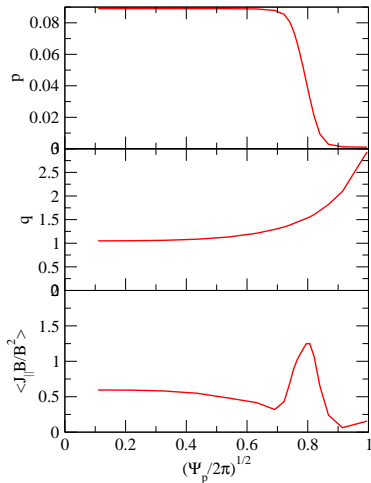
Outline

1. Nonlinear ballooning equations
 - ▶ Formulation
 - ▶ Analytic solution
2. Comparison with NIMROD simulations
 - ▶ Simulation setup
 - ▶ Comparison method
 - ▶ Comparison results
3. Summary and Discussion

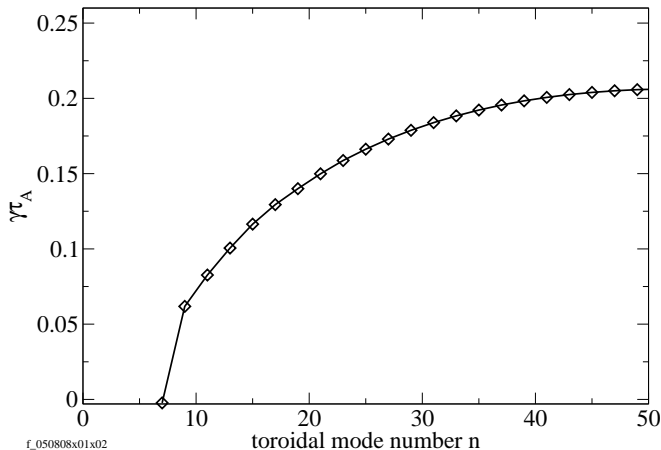
Simulations of ballooning instability are performed in a tokamak equilibrium with circular boundary and pedestal-like pressure



- ▶ Equilibrium from ESC solver [Zakharov and Pletzer, 1999].
- ▶ Finite element mesh in NIMROD [Sovinec *et al.*, 2004] simulation.

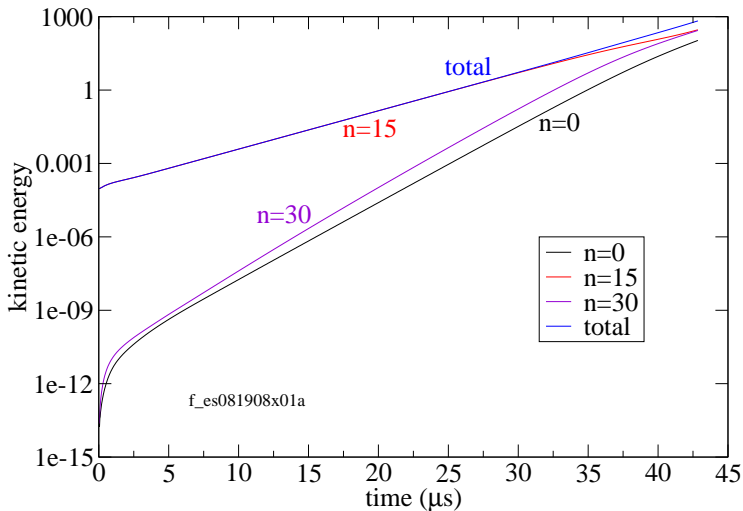


Linear ballooning dispersion is characteristic of interchange type of instabilities

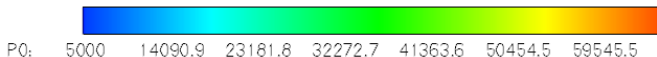
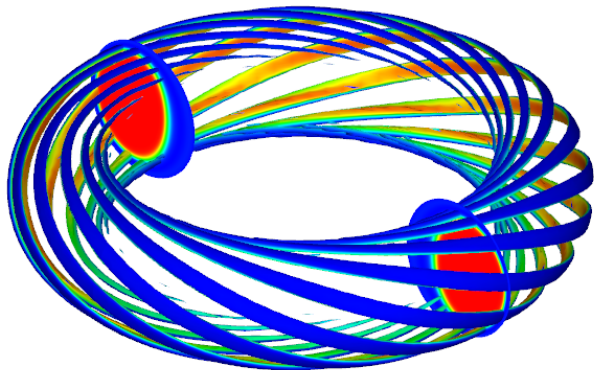


- ▶ Extensive benchmarks between NIMROD and ELITE show good agreement [B. Squires et al., Poster K1.00054, Sherwood 2009].

Simulation starts with a single $n = 15$ linear ballooning mode



Isosurfaces of perturbed pressure δp show
filamentary structure ($t = 30\mu s$, $\delta p = 168 Pa$)



For theory comparison, we need to know plasma displacement ξ associated with nonlinear ballooning instability

- ▶ ξ connects the Lagrangian and Eulerian frames,

$$\mathbf{r}(\mathbf{r}_0, t) = \mathbf{r}_0 + \boldsymbol{\xi}(\mathbf{r}_0, t) \quad (19)$$

- ▶ In the Lagrangian frame

$$\frac{d\boldsymbol{\xi}(\mathbf{r}_0, t)}{dt} = \mathbf{u}(\mathbf{r}_0, t) \quad (20)$$

- ▶ In the Eulerian frame

$$\partial_t \boldsymbol{\xi}(\mathbf{r}, t) + \mathbf{u}(\mathbf{r}, t) \cdot \nabla \boldsymbol{\xi}(\mathbf{r}, t) = \mathbf{u}(\mathbf{r}, t) \quad (21)$$

- ▶ ξ is advanced as an extra field in NIMROD simulations.

Lagrangian compression $\nabla_0 \cdot \xi$ can be more conveniently used to identify nonlinear regimes

- ▶ Nonlinearity is defined by $\varepsilon = |\xi|/L_{\text{eq}}$, but L_{eq} is not specific.
- ▶ Linear regime ($\varepsilon \ll n^{-1}$)

$$\nabla_0 \cdot \xi = \nabla \cdot \xi \ll 1 \quad (22)$$

- ▶ Early nonlinear regime ($\varepsilon \sim n^{-1}$)

$$\begin{aligned} \nabla_0 \cdot \xi &\sim \lambda_{\Psi}^{-1} \xi^{\Psi} + \lambda_{\alpha}^{-1} \xi^{\alpha} + \lambda_{\parallel}^{-1} \xi^{\parallel} \\ &\sim n^{1/2} n^{-1} + n^1 n^{-3/2} + n^0 n^{-1} \sim n^{-1/2} \ll 1. \end{aligned} \quad (23)$$

- ▶ Intermediate nonlinear regime ($\varepsilon \sim n^{-1/2}$)

$$\begin{aligned} \nabla_0 \cdot \xi &\sim \lambda_{\Psi}^{-1} \xi^{\Psi} + \lambda_{\alpha}^{-1} \xi^{\alpha} + \lambda_{\parallel}^{-1} \xi^{\parallel} \\ &\sim n^{1/2} n^{-1/2} + n^1 n^{-1} + n^0 n^{-1/2} \sim 1. \end{aligned} \quad (24)$$

The Lagrangian compression $\nabla_0 \cdot \xi$ is calculated from the Eulerian tensor $\nabla \xi$ in simulations

Transforming from Lagrangian to Eulerian frames, one finds

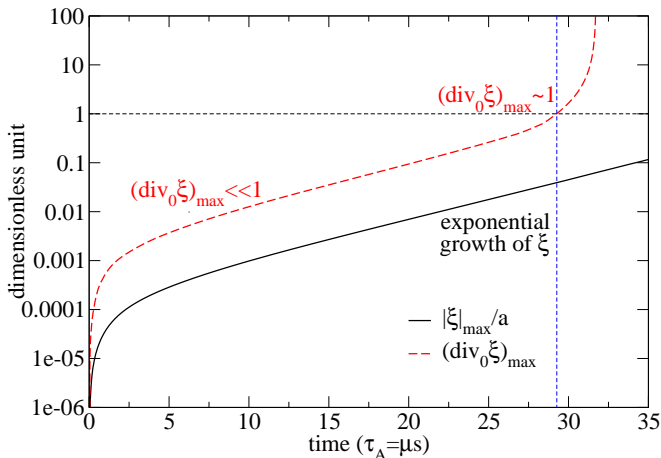
$$\xi(\mathbf{r}_0, t) = \xi[\mathbf{r} - \xi(\mathbf{r}, t), t] \quad (25)$$

$$\begin{aligned} \nabla \xi &= \frac{\partial \xi}{\partial \mathbf{r}} \\ &= \left(\frac{\partial \mathbf{r}}{\partial \mathbf{r}} - \frac{\partial \xi}{\partial \mathbf{r}} \right) \cdot \frac{\partial \xi}{\partial \mathbf{r}_0} \\ &= (\mathbf{I} - \nabla \xi) \cdot \nabla_0 \xi \end{aligned} \quad (26)$$

The Lagrangian compression $\nabla_0 \cdot \xi$ is calculated from the Eulerian tensor $\nabla \xi$ at each time step using

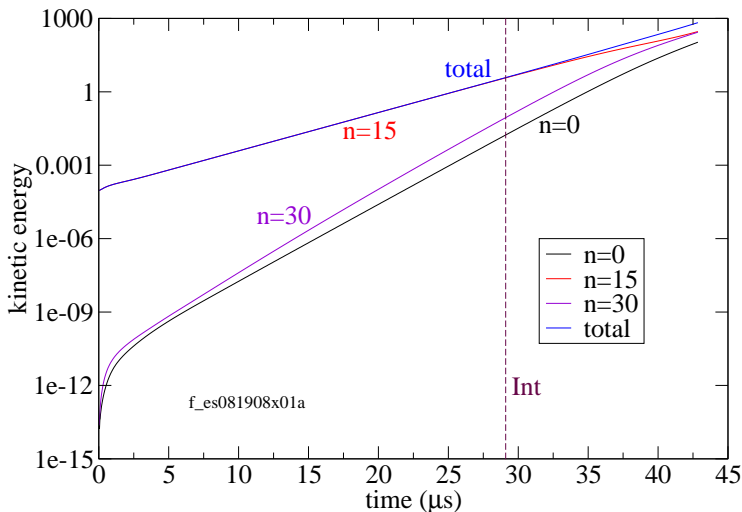
$$\nabla_0 \cdot \xi = \text{Tr}(\nabla_0 \xi) = \text{Tr}[(\mathbf{I} - \nabla \xi)^{-1} \cdot \nabla \xi]. \quad (27)$$

Exponential linear growth persists in the intermediate nonlinear regime of tokamak ballooning instability [Zhu, Hegna, and Sovinec, 2008]

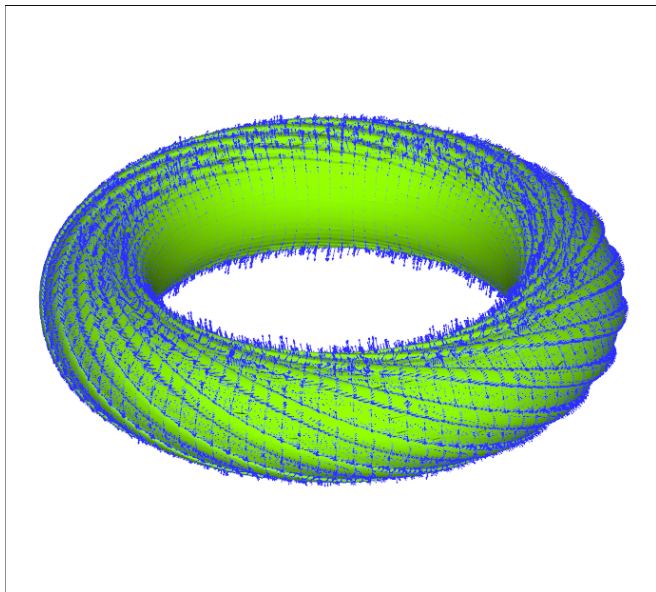


Dotted lines indicate the transition to the intermediate nonlinear regime when $\nabla_0 \cdot \xi \sim \mathcal{O}(1)$.

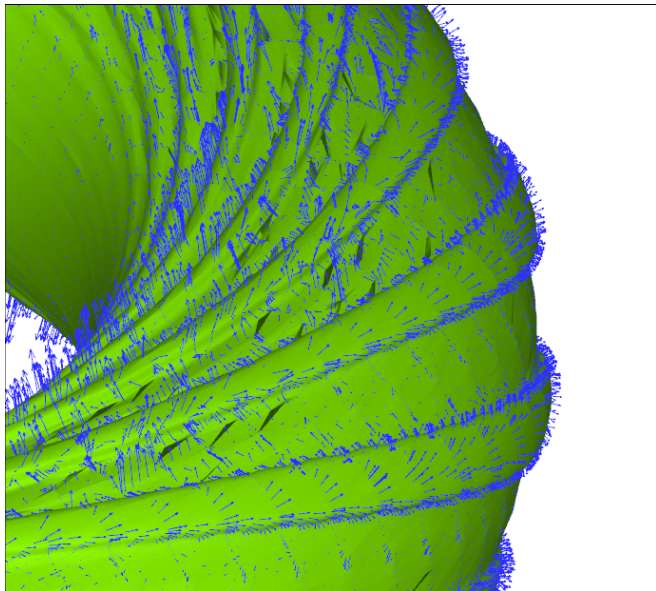
Perturbation energy grows with the linear growth rate into the intermediate nonlinear regime (vertical line)



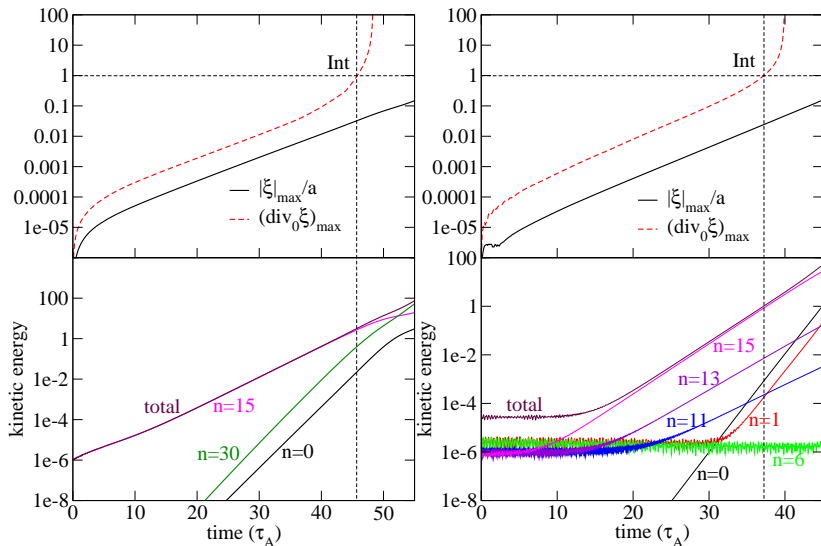
Distribution of plasma displacement vectors (ξ)
aligns with pressure isosurface ribbons ($t = 40\mu s$)



Distribution of plasma displacement vectors (ξ) aligns with pressure isosurface ribbons ($t = 40\mu s$)



Simulations started from multiple linear ballooning modes also confirm theory prediction



Summary

- ▶ There is an exponential growth phase in the nonlinear development of ballooning instability
 - ▶ The growth rate is same as the dominant linear component.
 - ▶ The spatial structure is same as the linear mode in Lagrangian space.
 - ▶ This nonlinear phase can be characterized by ordering $\xi_\psi \sim \lambda_\psi$ or $\nabla_0 \cdot \xi \sim \mathcal{O}(1)$.
 - ▶ During this nonlinear ballooning phase, radial convection and parallel dynamics appear to be independent.

Summary

- ▶ There is an exponential growth phase in the nonlinear development of ballooning instability
 - ▶ The growth rate is same as the dominant linear component.
 - ▶ The spatial structure is same as the linear mode in Lagrangian space.
 - ▶ This nonlinear phase can be characterized by ordering $\xi_\psi \sim \lambda_\psi$ or $\nabla_0 \cdot \xi \sim \mathcal{O}(1)$.
 - ▶ During this nonlinear ballooning phase, radial convection and parallel dynamics appear to be independent.
- ▶ Implications
 - ▶ May correspond to the initial nonlinear phase of the ELM precursor or ELM itself.
 - ▶ May explain the persistence of ELM filaments in both experiments and simulations.

Open question: How does the nonlinear ballooning instability lead to the onset of ELMs?

- ▶ Question: is nonlinear ballooning responsible for ELM precursor, or ELM itself, or both?
 - ▶ Late nonlinear regimes: saturation, precursor -> onset, filament -> blob?
 - ▶ Marginally unstable configuration ($\Gamma \sim 0$) -> “detonation regime” [Wilson and Cowley, 2004] -> ELM trigger?

Open question: How does the nonlinear ballooning instability lead to the onset of ELMs?

- ▶ Question: is nonlinear ballooning responsible for ELM precursor, or ELM itself, or both?
 - ▶ Late nonlinear regimes: saturation, precursor -> onset, filament -> blob?
 - ▶ Marginally unstable configuration ($\Gamma \sim 0$) -> “detonation regime” [Wilson and Cowley, 2004] -> ELM trigger?
- ▶ Other effects/complications:
 - ▶ 2-fluid, FLR (finite Larmor radius) effects
 - ▶ Edge shear flow effects
 - ▶ RMP (resonant magnetic perturbation) effects
 - ▶ Geometry (non-circular shape, divertor separatrix/X-point)
 - ▶ Nonlinear peeling-ballooning coupling
 - ▶